Strong coupling of polaritons at room temperature in a GaAs/AlGaAs structure

Hassan Alnatah,[1,*,†] Shuang Liang,[1,*] Qiaochu Wan,[1] Jonathan Beaumariage,[1] Ken West,[2] Kirk Baldwin,[2] Loren N. Pfeiffer,[2] Man Chun Alan Tam,[3,4] Zbigniew R. Wasilewski,[3,4,5] and David W. Snoke[1]

[1]*Department of Physics, University of Pittsburgh, 3941 O'Hara Street, Pittsburgh, Pennsylvania 15218, USA*

[2]*Department of Electrical Engineering, Princeton University, Princeton, New Jersey 08544, USA*

[3]*Department of Electrical and Computer Engineering, University of Waterloo, Waterloo, Ontario, Canada*

[4]*Waterloo Institute for Nanotechnology, University of Waterloo, Waterloo, Ontario, Canada*

[5]*The Institute for Quantum Computing (IQC), University of Waterloo, Waterloo, Ontario, Canada*

(Received 13 May 2025; accepted 18 June 2025; published 7 July 2025)

We report direct measurement of the dispersion relation of polaritons in GaAs/AlGaAs microcavity structures at room temperature, which clearly shows that the polaritons are in the strong-coupling limit. The Rabi splitting ranges from 12.3 to 15.2 meV depending on the detuning, significantly exceeding the heavy-hole exciton half width of 5.2 meV. As the polariton density increases, the Rabi splitting decreases; but even when the polariton gas becomes a coherent, Bose-condensate-like state, the polaritons retain a strong exciton component, as seen in the nonlinear energy shift of the light emission. This opens up the possibility of polaritonic devices at room temperature in a material system which can be grown with very high quality and uniformity.

DOI: 10.1103/dstp-cbcf

I. INTRODUCTION

Polaritons can be viewed as photons dressed with an effective mass and repulsive interactions, due to the strong coupling of a cavity photon state and a semiconductor exciton state. Over the past two decades, numerous experiments have demonstrated Bose condensation and nonlinear coherent effects in GaAs/AlGaAs structures at cryogenic temperatures (e.g., [1–6]). Strong coupling occurs when the Rabi splitting is larger than the half widths of the states, implying that the vacuum oscillation rate between the exciton and photon modes is faster than their decay times.

Polaritonic strong coupling at room temperature is desirable to use their strong optical nonlinearity for practical polaritonic devices. Polaritons in the strong-coupling limit have been seen in organic materials [7–9] and perovskites [10,11]. Significant efforts have also been made to achieve strong coupling in III-V structures at room temperature. Earlier results [12–14] had spectral half widths comparable to, or only slightly smaller than, the measured Rabi splittings. Furthermore, none of these earlier works above showed a nonlinear shift of the spectral lines, line narrowing, or lasing as the excitation density increased. While a nonlinear line shift is not a direct indicator of strong coupling, it indicates that the polaritons have a significant excitonic fraction, and is essential for nonlinear optical applications.

In a previous paper, we reported polaritonic coherent emission at room temperature in GaAs/AlGaAs microcavity structures [15]. A thermalized energy distribution was seen and it was clear that polaritonic effects involving an exciton fraction were present, as seen in the strong energy shift of the emission line with pump power. However, at that time, it was not clear what exciton fraction could be attributed to the polaritons; it was argued in Ref. [15] that the coupling of the photons to excitons was weak but nonzero, with exciton fraction of 10% or less, based on a model of the photon-exciton coupling using the observed photoluminescence (PL) data.

We have now performed similar experiments with multiple structures with different designs, with different designed Q factors of the cavities and different numbers of quantum wells, and a wide range of pumping conditions. Crucially, by looking at a sample with lower Q factor of the microcavity, we can easily observe three polariton branches arising from the heavy-hole exciton, light-hole exciton, and cavity photon mode, which allows us to fit the entire dispersion curves of the polaritons.

In this work, we demonstrate a Rabi splitting of approximately 13 meV at room temperature, which is more than twice the heavy-hole exciton half width of 5.2 meV. We find that in all of the studied samples, the polaritons are in strong coupling at low pump power at room temperature, and remain in relatively strong coupling as the pump power is increased into the coherent emission regime. The Rabi splitting decreases as density increases, but never fully collapses to zero, as far as we can measure.

This result is surprising, but is a result of the fact that our samples have very sharp exciton lines in the quantum wells even at room temperature. (The Supplemental Material [16] shows the exciton emission from bare quantum wells grown using the same process but without a microcavity.) When the quantum wells are embedded in a microcavity, we expect that there will be splitting of the excitons into multiple states due to well-width fluctuations, but this does not imply broadening of the exciton-polariton lines. The line width of polariton states primarily arises from the homogeneous broadening of the exciton states and is not strongly affected by the presence of multiple exciton states.

*These authors contributed equally to this work.
†Contact author: haa108@pitt.edu

TABLE I. Sample designs with different quantum-well (QW) numbers, top DBR periods, and Rabi splitting values derived from fits to the dispersion data near resonance. All samples have the same number of periods of the bottom DBR. Samples labeled P were grown in the Pfeiffer laboratory at Princeton University, while the sample labeled W was grown at the Wasilewski Laboratory at the University of Waterloo.

Sample name	No. QWs	Periods of Top DBR	Rabi Splitting (meV)
Sample P1	12	23	12.41 ± 0.08
Sample P2	12	29	12.57 ± 0.14
Sample P3	12	32	13.21 ± 0.54
Sample W1	28	32	13.33 ± 0.12

II. EXPERIMENTAL METHODS

In the experiments reported here, we used a GaAs/AlGaAs microcavity structure very similar to those of previous experiments [15,17,18]. We have used four different samples throughout this work. Table I summarizes their properties. Three of the four samples consisted of a total of 12 GaAs quantum wells with AlAs barriers embedded within a distributed Bragg reflector (DBR), with each sample having a different number of periods of the top DBR. The fourth sample, in contrast, consisted of a total of 28 GaAs quantum wells. In all samples, the quantum wells are in groups of four, with each group placed at one of the antinodes of the cavity. Further details about the samples are discussed in the Supplemental Material [16].

All the measurements reported in this paper and Supplemental Material [16] were at room temperature, with no cryogenic system. The polaritons were generated by pumping the sample nonresonantly with a wavelength-tunable laser, tuned to a reflectivity minimum (737.4 nm) approximately 172 meV above the lower polariton resonance. To minimize heating of the sample, the pump laser was modulated using an optical chopper with a duty cycle of 1% and pulses of duration approximately 25 μs, which is very long compared to the dynamics of the system. The nonresonant pump created electrons and holes, which scattered down in energy to become polaritons. The photoluminescence (PL) was collected

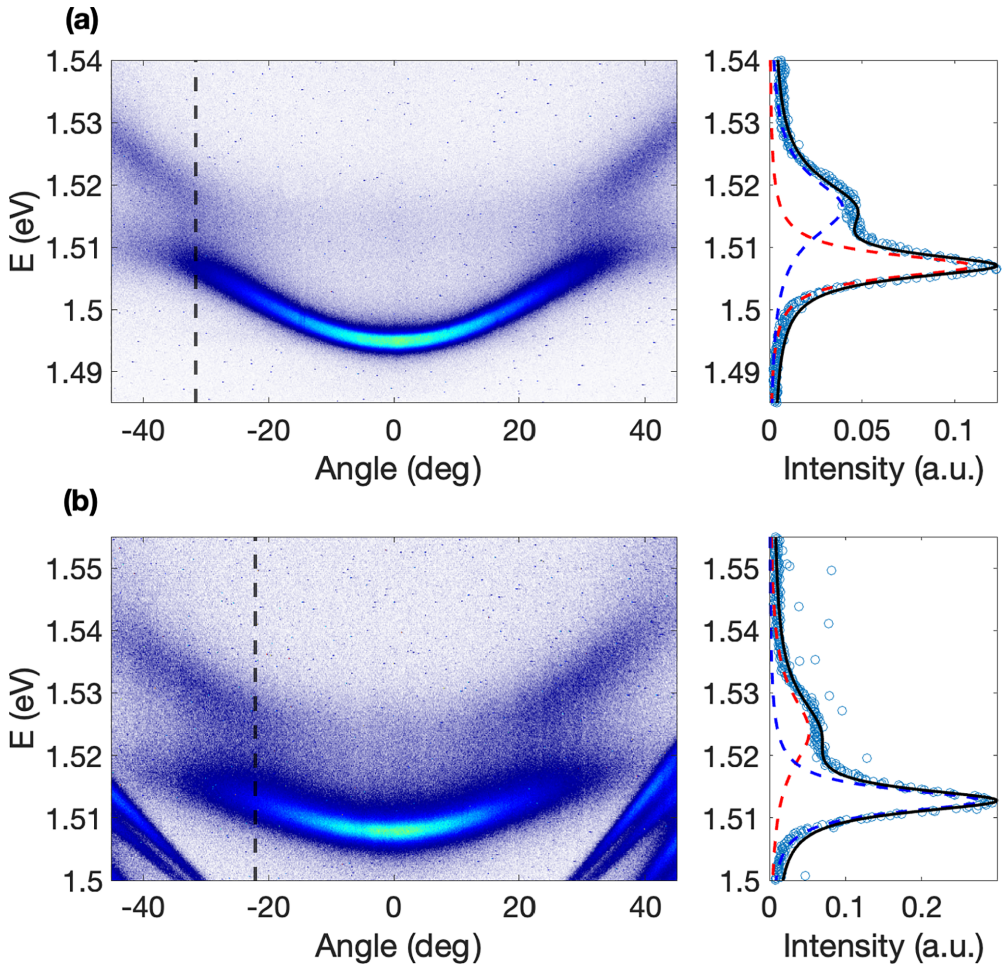

FIG. 1. Strong coupling at room temperature in samples P1 and W1. (a) Left plot: angle-resolved PL measurements of the polariton at very low pumping power for sample P1 at a location with LP exciton fraction of approximately 0.12 at $k = 0$. Right plot: the intensity as a function of energy along the slice at constant angle corresponding to the vertical dashed line in (a). To reduce the noise in the experimental data, we averaged over 20 pixels around the slice. Dashed lines: fit to two Lorentzian peaks. (b) The same measurements at very low pumping power for sample W1, for an LP exciton fraction of approximately 0.24 at $k = 0$. The extra curved lines seen at low energy and high angle in (b) are ripples in the reflectivity spectrum at the edge of the stop band of the DBR cavity of this sample.

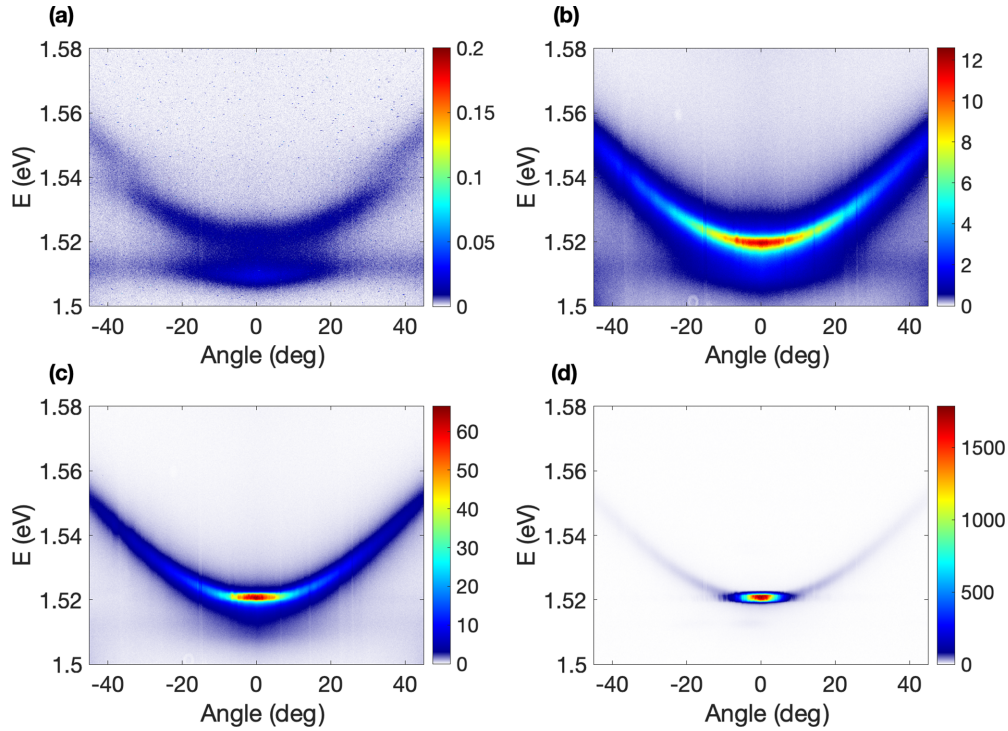

FIG. 2. Angle-resolved PL for different pump powers, at a location on sample P1 with 0.54 exciton fraction of the LP at $k = 0$. (a) Pump power $P = 0.01P_{\text{th}}$, (b) $P = 0.83P_{\text{th}}$, (c) $P = 1.00P_{\text{th}}$, and (d) $P = 1.13P_{\text{th}}$. The threshold power P_{th} is defined in Sec. III of the Supplemental Material [16].

using a microscope objective with a numerical aperture of 0.75 and was imaged onto the entrance slit of a spectrometer. The image was then sent through the spectrometer to a CCD camera for time-integrated imaging.

To measure the energy dispersion of the polaritons, we used angle-resolved photoluminscence (PL) to obtain the intensity image $I(\theta, E)$, where θ is the angle of emission, which has a one-to-one mapping to the in-plane momentum of the polaritons. The angle of photon emission maps directly to the in-plane k vector of the particles inside the structure. The exciton fraction can be chosen by moving to different locations on the sample, where the cavity photon energy varies because of the thickness gradient across the wafer. This thickness variation causes a change in cavity photon energy, as the wavelength of the photon inside the cavity is proportional to the cavity length.

III. EXPERIMENTAL RESULTS

Figure 1 shows examples of dispersion of the polaritons measured at room temperature for two different samples, clearly demonstrating strong coupling with two distinct polariton branches. These branches, lower polariton (LP) and middle polariton (MP), arise due to the interaction between the heavy-hole exciton with the cavity photon mode.

Polariton condensation was observed as we increased the pump power across the phase transition. Figure 2 shows angle-resolved PL for different pump powers for the case of the LP mode near resonance with the cavity photon. In this case, the higher, light-hole exciton branch is clearly visible. As is typical for polariton condensation, the PL narrows both in k space and in energy width as the density increases; the latter indicates coherence of the emission. We note that at room temperature, the two lowest polariton modes are roughly equally occupied and therefore the lowest-energy state is not strongly favored.

The linewidths and the energy positions of the polariton lines were extracted from the $I(\theta, E)$ images by taking a vertical slice at $\theta = 0$ to obtain $I(E)$. The resulting intensity profiles were fitted to the sum of two Lorentzians, corresponding to the LP and MP. The upper polariton (UP), being very excitonic at $\theta = 0$, was essentially undetectable except at the anticrossing regions, as seen in Fig. 2. Since the detuning in Fig. 2 corresponds to the case of approximately 0.5 exciton fraction of the LP and MP, the difference between the peak positions of the two Lorentzians extracted from the fits, plotted in Fig. 3(c), is close to the Rabi splitting energy. Because this is a three-level system with contribution from the light-hole exciton state, the cavity photon does not lie exactly in the middle of the LP and MP states, and the splitting there is not exactly equal to the Rabi energy.

As the pump power is increased, the LP and MP lines shift but remain resolvable up to the onset of strong coherence, indicated by line narrowing and a jump in the emission intensity. At high power, only a single peak is resolvable. Above this power, we used a single Lorentzian fit to extract the linewidth and energy shift (denoted by the filled black circles). Above the density indicated by the vertical dashed lines in Fig. 3, the system appears to collapse to weak coupling, i.e., photonic condensation.

The Rabi splitting at very low pumping power, extracted from the three-level model described below (with parameters provided in the Supplemental Material [16]), ranges from

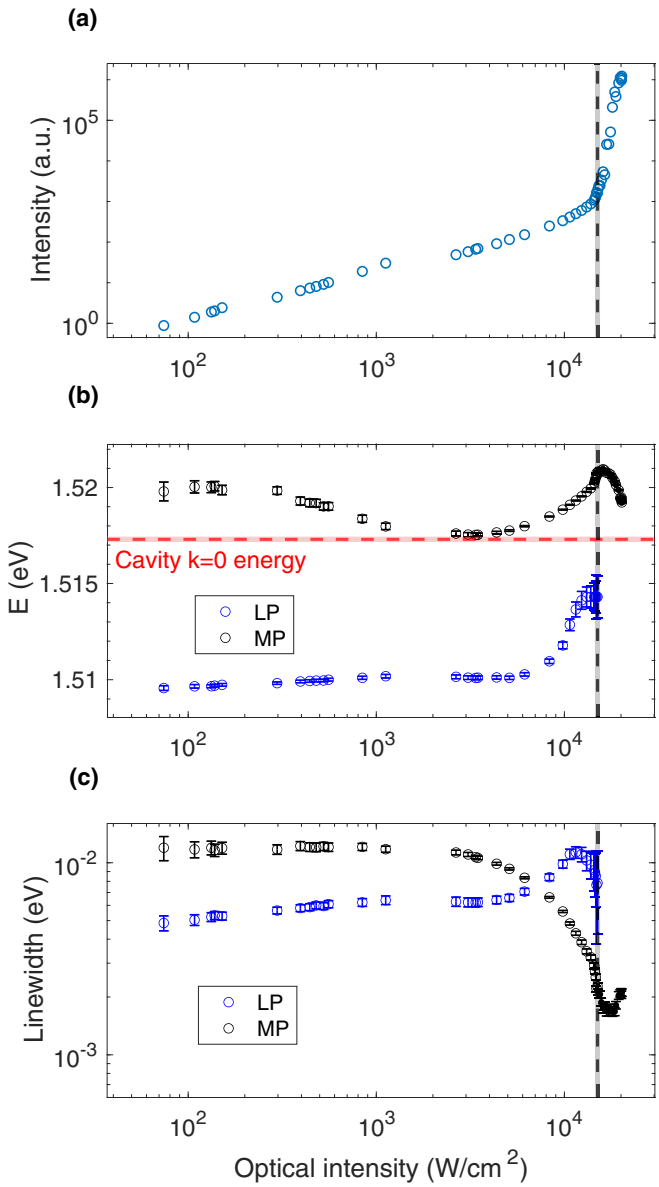

FIG. 3. Blueshift and linewidth of the PL lines for sample P1 at a location with 0.54 LP exciton fraction at $k = 0$. (a) The intensity at $k = 0$ of the polaritons as a function of optical pump intensity, corrected for the reflection from the top surface. (b) The energies of the polariton lines at $k = 0$ as a function of the pump power. The red dashed line represents the zero-energy cavity extracted from the three-level model fits. The line marked "Cavity $k = 0$ energy" is the value from the fit of Fig. 4(b); the vertical pink range gives the uncertainty of this value. The bare heavy-hole exciton energy is very near to this value. (c) Circles: Full width at half maximum at $k = 0$. A single Lorentzian fit was used for the data corresponding to solid circles since we see only main peaks at high power due to condensation. The vertical black dashed lines (with uncertainty given by the gray regions) indicate the power beyond which the system can no longer be identified as being in the strong-coupling regime.

12.3 to 15.2 meV, depending on the detuning. The three-level model is highly constrained, as it fits the full energy dispersion for different emission angles and all three polariton branches (upper, middle, and lower). The Rabi splitting values are directly obtained from such fits, as illustrated in Fig. 4.

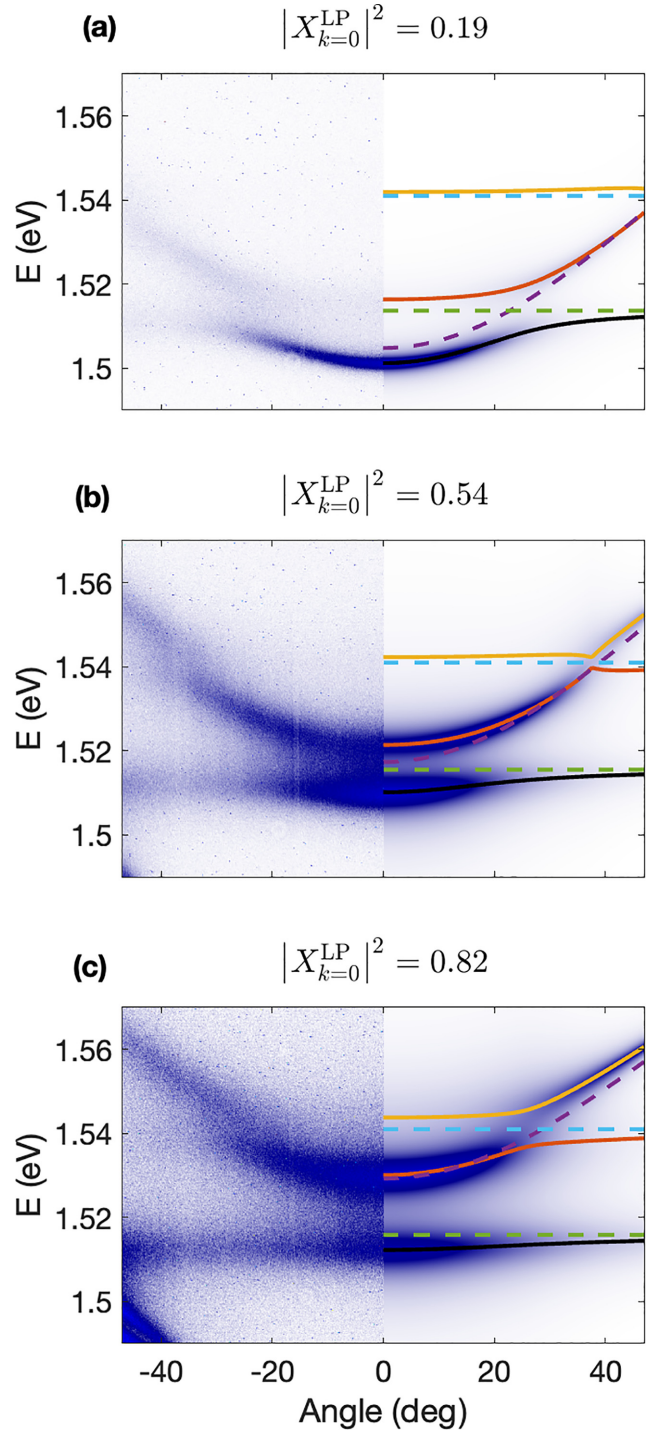

FIG. 4. Angle-resolved PL for different locations on sample P1 compared to simulation. Left side of each image: Angle-resolved PL measurements of the polariton at very low pumping power, corresponding to the estimated exciton fractions of the lower polariton at $k = 0$ given by the upper labels. Right sides: simulated data using the model discussed in the text. The parameters for the fits are given in the Supplemental Material [16]. The solid black, red, and yellow lines represent the LP, MP, and UP, respectively. The green dashed line represents the heavy-hole exciton energy, the blue dashed line represents the light-hole exciton energy, and the purple dashed line represents the cavity energy. The extra curved lines seen at low energy and high angle in (c) are ripples in the reflectivity spectrum at the edge of the stop band of the DBR cavity of this sample.

The obtained values from the fits of Rabi splitting are significantly larger than the heavy-hole exciton half width, measured to be approximately 5.2 meV, yielding a ratio of $\Omega_{hh}/\Gamma_{hh} \approx 2.3$–$2.9$—about a factor of two above the highest value reported in previous work, where $\Omega_{hh}/\Gamma_{hh} \approx 1$–$1.2$ [12–14]. This improvement in achieving a larger Ω_{hh}/Γ_{hh} is not merely a technical enhancement, but also enables the system to maintain strong coupling at higher pumping powers. As a result, strong coupling persists well into the nonlinear regime (as shown in Fig. 3), where significant blueshift of the lower polariton line is observed, before eventually becoming weak coupling at higher pumping powers.

As shown in Fig. 3, the coherence is accompanied by a nonmonotonic energy shift, indicating substantial interactions present in the system and, therefore, strong nonlinearity. Above the threshold density for weak coupling, the blueshift is reversed, as the polaritons appear to be pulled back down to the bare cavity photon energy. In this same regime, the line broadens again, indicating that the system is becoming less coherent.

IV. ANALYSIS

A simple three-level model for our GaAs-based microcavity structures incorporating photons, heavy-hole excitons, and light-hole excitons can be expressed as follows:

$$H(\theta) = \begin{pmatrix} E_{cav}(\theta) + i\Gamma_{cav} & \Omega/2 & \Omega/2 \\ \Omega/2 & E_{hh} + i\Gamma_{hh} & 0 \\ \Omega/2 & 0 & E_{lh} + i\Gamma_{lh} \end{pmatrix}, \quad (1)$$

where Γ_{cav} gives the half width at half maximum of the photon linewidth broadening, which is negligible compared to the exciton linewidths in our samples, and Γ_{hh} and Γ_{lh} give the heavy-hole and light-hole exciton broadening. We diagonalized the Hamiltonian for each θ value to obtain the real and imaginary parts of its eigenvalues. The imaginary parts correspond to the half widths of the polaritons. This then allowed us to compute a simulated $I(\theta, E)$ image by summing three Lorentzians, each representing the LP, MP, and UP. The real parts of the Hamiltonian eigenvalues give the Lorentzian peaks, while the imaginary parts give their half widths. We ensured that the integral of each Lorentzian at each θ slice is equal to the Maxwell-Boltzmann distribution $e^{-[E(\theta)-E_{LP}(\theta=0)]/k_BT}$. Finally, to account for the radiative lifetime of the polaritons, we scaled each Lorentzian by the photon fraction since the more photonic the polariton is, the more likely it is to emit a photon outside the cavity.

Figure 4 shows the simulations of the three-level model alongside the experimental data for different locations on the sample. The simulations successfully capture the key features observed in the experimental data, giving a similar dispersion and linewidth of the polaritons. This strong agreement highlights the effectiveness of the three-level model in capturing the essential physics governing the system. For photonic detunings, the light-hole exciton intersects the cavity mode at a larger angle than what we can collect with our numerical aperture, making the upper polariton not visible.

As discussed in the Supplemental Material [16], the transition from strong coupling to weak coupling seen at higher densities can be understood in terms of a classical dielectric model. In both limits, i.e., strong coupling and weak coupling, the nonlinear shift of the lines can be understood as an effect of the mixing of the exciton and photon states.

V. CONCLUSIONS

The clear observation of strong coupling in a GaAs/AlGaAs structure is surprising because the binding energy of excitons in quantum wells in this material system is only around 10 meV [19], well below the thermal energy $k_BT = 25.7$ meV. This implies that there will be a significant population of free electrons and holes, which can lead to complicated renormalization of the energies of the states, but as seen clearly in these experiments, the free electrons and holes do not screen out the exciton resonance at low densities.

In the case of the resonant detuning shown here, the system clearly remains in strong coupling even as the PL line narrows into the coherent regime, until a density threshold is exceeded at which it appears to collapse to weak coupling. At detunings far from resonance, the system collapses to weak coupling at densities below the onset of coherence, but even in those cases, the exciton/electron-hole optical resonance still gives a strong interaction of the photons with excitons. This nonlinear interaction gives nonmonotonic energy shifts of the emission energy in all cases. This may be useful for nonlinear optical switching applications at room temperature.

These results imply that there is potential to make exciton-polariton-based GaAs/AlGaAs devices for room-temperature applications, including low-threshold lasers and nonlinear optical devices.

ACKNOWLEDGMENT

This project has been supported by the National Science Foundation Grant No. DMR-2306977.

DATA AVAILABILITY

The data that support the findings of this article are openly available [20]; embargo periods may apply.

[1] H. Deng, G. Weihs, C. Santori, J. Bloch, and Y. Yamamoto, Condensation of semiconductor microcavity exciton polaritons, Science **298**, 199 (2002).

[2] J. Kasprzak, M. Richard, S. Kundermann, A. Baas, P. Jeambrun, J. M. J. Keeling, F. Marchetti, M. Szymańska, R. André, J. Staehli *et al.*, Bose-Einstein condensation of exciton polaritons, Nature (London) **443**, 409 (2006).

[3] R. Balili, V. Hartwell, D. Snoke, L. Pfeiffer, and K. West, Bose-Einstein condensation of microcavity polaritons in a trap, Science **316**, 1007 (2007).

[4] M. Abbarchi, A. Amo, V. Sala, D. Solnyshkov, H. Flayac, L. Ferrier, I. Sagnes, E. Galopin, A. Lemaître, G. Malpuech *et al.*, Macroscopic quantum self-trapping and Josephson oscillations of exciton polaritons, Nat. Phys. **9**, 275 (2013).

[5] D. Sanvitto, F. Marchetti, M. Szymańska, G. Tosi, M. Baudisch, F. P. Laussy, D. Krizhanovskii, M. Skolnick, L. Marrucci, A. Lemaitre *et al.*, Persistent currents and quantized vortices in a polariton superfluid, Nat. Phys. **6**, 527 (2010).

[6] K. Lagoudakis, T. Ostatnickỳ, A. Kavokin, Y. G. Rubo, R. André, and B. Deveaud-Plédran, Observation of half-quantum vortices in an exciton-polariton condensate, Science **326**, 974 (2009).

[7] J. D. Plumhof, T. Stöferle, L. Mai, U. Scherf, and R. F. Mahrt, Room-temperature Bose-Einstein condensation of cavity exciton-polaritons in a polymer, Nat. Mater. **13**, 247 (2014).

[8] M. Dusel, S. Betzold, O. A. Egorov, S. Klembt, J. Ohmer, U. Fischer, S. Höfling, and C. Schneider, Room temperature organic exciton-polariton condensate in a lattice, Nat. Commun. **11**, 2863 (2020).

[9] M. Wei, W. Verstraelen, K. Orfanakis, A. Ruseckas, T. C. Liew, I. D. Samuel, G. A. Turnbull, and H. Ohadi, Optically trapped room temperature polariton condensate in an organic semiconductor, Nat. Commun. **13**, 7191 (2022).

[10] R. Su, S. Ghosh, J. Wang, S. Liu, C. Diederichs, T. C. Liew, and Q. Xiong, Observation of exciton polariton condensation in a perovskite lattice at room temperature, Nat. Phys. **16**, 301 (2020).

[11] R. Su, J. Wang, J. Zhao, J. Xing, W. Zhao, C. Diederichs, T. C. Liew, and Q. Xiong, Room temperature long-range coherent exciton polariton condensate flow in lead halide perovskites, Sci. Adv. **4**, eaau0244 (2018).

[12] S. Tsintzos, P. Savvidis, G. Deligeorgis, Z. Hatzopoulos, and N. Pelekanos, Room temperature gaas exciton-polariton light emitting diode, Appl. Phys. Lett. **94**, 071109 (2009).

[13] S. Brodbeck, J.-P. Jahn, A. Rahimi-Iman, J. Fischer, M. Amthor, S. Reitzenstein, M. Kamp, C. Schneider, and S. Höfling, Room temperature polariton light emitting diode with integrated tunnel junction, Opt. Express **21**, 31098 (2013).

[14] H. Suchomel, S. Kreutzer, M. Jörg, S. Brodbeck, M. Pieczarka, S. Betzold, C. Dietrich, G. Sęk, C. Schneider, and S. Höfling, Room temperature strong coupling in a semiconductor microcavity with embedded AlGaAs quantum wells designed for polariton lasing, Opt. Express **25**, 24816 (2017).

[15] H. Alnatah, S. Liang, Q. Yao, Q. Wan, J. Beaumariage, K. West, K. Baldwin, L. N. Pfeiffer, and D. W. Snoke, Bose-Einstein condensation of polaritons at room temperature in a GaAs/AlGaAs structure, ACS Photon. **12**, 48 (2024).

[16] See Supplemental Material at http://link.aps.org/supplemental/10.1103/dstp-cbcf for additional angle-resolved data, measurements of exciton energies and linewidths, the parameters used in the three-level model, and a classical dielectric model that simulates the transition from strong to weak coupling. The Supplemental Material also contains Refs. [21–28].

[17] H. Alnatah, Q. Yao, J. Beaumariage, S. Mukherjee, M. C. Tam, Z. Wasilewski, K. West, K. Baldwin, L. N. Pfeiffer, and D. W. Snoke, Coherence measurements of polaritons in thermal equilibrium reveal a power law for two-dimensional condensates, Sci. Adv. **10**, eadk6960 (2024).

[18] H. Alnatah, P. Comaron, S. Mukherjee, J. Beaumariage, L. N. Pfeiffer, K. West, K. Baldwin, M. Szymańska, and D. W. Snoke, Critical fluctuations in a confined driven-dissipative quantum condensate, Sci. Adv. **10**, eadi6762 (2024).

[19] G. Bastard, E. E. Mendez, L. L. Chang, and L. Esaki, Exciton binding energy in quantum wells, Phys. Rev. B **26**, 1974 (1982).

[20] H. Alnatah, S. Liang, Q. Wan, J. Beaumariage, K. West, K. Baldwin, L. Pfeiffer, M. C. A. Tam, Z. Wasilewski, and D. Snoke, Data for strong coupling of polaritons at room temperature in a GaAs/AlGaAs structure, Zenodo (2025), doi:10.5281/zenodo.15400412.

[21] M. Pieczarka, M. Gębski, A. N. Piasecka, J. A. Lott, A. Pelster, M. Wasiak, and T. Czyszanowski, Bose-Einstein condensation of photons in a vertical-cavity surface-emitting laser, Nat. Photon. **18**, 1090 (2024).

[22] H. Deng, G. Weihs, D. Snoke, J. Bloch, and Y. Yamamoto, Polariton lasing vs. photon lasing in a semiconductor microcavity, Proc. Natl. Acad. Sci. **100**, 15318 (2003).

[23] D. Caputo, D. Ballarini, G. Dagvadorj, C. Sánchez Muñoz, M. De Giorgi, L. Dominici, K. West, L. N. Pfeiffer, G. Gigli, F. P. Laussy *et al.*, Topological order and thermal equilibrium in polariton condensates, Nat. Mater. **17**, 145 (2018).

[24] B. Nelsen, G. Liu, M. Steger, D. W. Snoke, R. Balili, K. West, and L. Pfeiffer, Dissipationless flow and sharp threshold of a polariton condensate with long lifetime, Phys. Rev. X **3**, 041015 (2013).

[25] D. W. Snoke, V. Hartwell, J. Beaumariage, S. Mukherjee, Y. Yoon, D. M. Myers, M. Steger, Z. Sun, K. A. Nelson, and L. N. Pfeiffer, Reanalysis of experimental determinations of polariton-polariton interactions in microcavities, Phys. Rev. B **107**, 165302 (2023).

[26] J. Beaumariage, Z. Sun, H. Alnatah, Q. Yao, D. M. Myers, M. Steger, K. West, K. Baldwin, L. N. Pfeiffer, M. C. A. Tam *et al.*, Measurement of exciton fraction of microcavity exciton-polaritons using transfer-matrix modeling, arXiv:2406.12940.

[27] J. A. Kash, Carrier-carrier scattering in GaAs: Quantitative measurements from hot (e, A^0) luminescence, Phys. Rev. B **40**, 3455 (1989).

[28] D. W. Snoke, W. W. Rühle, Y.-C. Lu, and E. Bauser, Evolution of a nonthermal electron energy distribution in GaAs, Phys. Rev. B **45**, 10979 (1992).